Ultrafast Non-Förster Intramolecular Donor−Acceptor Excitation Energy Transfer

Stavros Athanasopoulos,*[,†,‡] Laura Alfonso Hernandez,[§] David Beljonne,[∥] Sebastian Fernandez-Alberti,[§] and Sergei Tretiak[⊥]

[†]Departamento de Física, Universidad Carlos III de Madrid, Avenida Universidad 30, 28911 Leganés, Madrid, Spain
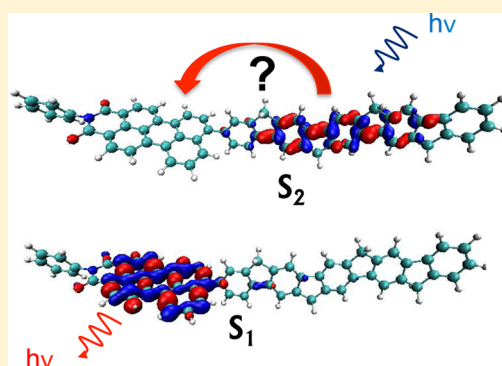[‡]Experimental Physics II, University of Bayreuth, Bayreuth 95440, Germany
[§]Universidad Nacional de Quilmes/CONICET, Roque Saenz Peña 352, B1876BXD Bernal, Argentina
[∥]Laboratory for Chemistry of Novel Materials, University of Mons, Place du Parc 20, B-7000 Mons, Belgium
[⊥]Theoretical Division, Center for Nonlinear Studies (CNLS) and Center for integrated Nanotechnologies (CINT), Los Alamos National Laboratory, Los Alamos, New Mexico 87545, United States

Ⓢ *Supporting Information*

ABSTRACT: Ultrafast intramolecular electronic energy transfer in a conjugated donor−acceptor system is simulated using nonadiabatic excited-state molecular dynamics. After initial site-selective photoexcitation of the donor, transition density localization is monitored throughout the $S_2 \rightarrow S_1$ internal conversion process, revealing an efficient unidirectional donor → acceptor energy-transfer process. Detailed analysis of the excited-state trajectories uncovers several salient features of the energy-transfer dynamics. While a weak temperature dependence is observed during the entire electronic energy relaxation, an ultrafast initially temperature-independent process allows the molecular system to approach the S_2−S_1 potential energy crossing seam within the first ten femtoseconds. Efficient energy transfer occurs in the absence of spectral overlap between the donor and acceptor units and is assisted by a transient delocalization phenomenon of the excited-state wave function acquiring Frenkel-exciton character at the moment of quantum transition.

Intramolecular energy transfer (ET) is a key photophysical process that takes place in a range of biological, biomimetic, and molecular systems.[1−5] The rate of energy transfer is controlled by the underlying chemical structure and surrounding environment, and it competes with radiative and nonradiative decay pathways. It is therefore important to funnel the excitation with a high efficiency to a place where the desired function takes place, i.e., convert light into chemical energy or electricity. For example, the ability to transfer the photoexcitation in acceptor sites is necessary for sensing applications and biological recognition processes.[6] Tailoring such energy-transfer processes in conjugated materials is critical for the operation and efficiency of organic optoelectronic devices.[7] In particular, exciton diffusion to donor−acceptor interfaces in photovoltaic blends is a prerequisite for charge generation and extraction.[8,9] Capturing an excitation at trapping sites found in conjugated polymers reduces the efficiency of the photovoltaic effect in organic solar cells,[10] while similar quenching mechanisms to nonradiative defect sites decrease the electroluminescent efficiency and are therefore detrimental for the operation of organic light-emitting diodes.[11] Förster resonance energy transfer (FRET) is commonly used to describe singlet ET between donor and acceptor units and as a molecular ruler for determining macromolecular distances spectroscopically.

The original formulation of FRET relies, among others, on the point dipole approximation, which requires that donor−acceptor distances are much larger than the sizes of the individual dipoles of the units,[12−14] and on coupling of the donor and acceptor electronic excitations to independent baths (see ref 15). In this formulation, efficient FRET occurs provided the donor and acceptor are coupled through a long-range Coulomb interaction and there is significant overlap between donor emission and acceptor absorption spectra.[16−19] However, for covalently bonded molecular systems, short-range interactions are enabled and can play a significant role in the energy-transfer process.[1,20]

Currently there is a lack of understanding of the dynamics of intramolecular energy transfer in bridged donor−acceptor systems.[20] Recent experiments have shown that although this process is fast, it cannot be described by the conventional FRET model. Moreover, efficient energy transfer can take place even in the absence of spectral overlap between the donor and acceptor molecules.[21,22] There are three distinct physical mechanisms that can contribute to the energy transfer in

molecular systems. These are (i) long-range resonance, or through-space ET, controlled by dipole−dipole coupling and treated within the Förster point dipole, extended dipole or multicentric monopole approximations;[23,24] (ii) short-range wave function overlap or through-bond mechanisms, included in the Dexter approximation (two-electron exchange interaction)[25] or accounted for by mixing the localized excitations with charge-transfer excitations (one-electron coupling); and (iii) superexchange bridge-mediated mechanisms.[26,27] The relevant contribution of each individual process is difficult to assess a priori, and at the theoretical level, often approximations are made that neglect certain contributions. Moreover, the influence of environment and vibrational dynamics[28] is often disregarded by treating the problem within a static picture of relaxed donor and acceptor units at their respective gas-phase ground- and excited-state geometries, respectively. However, nuclear motions induce changes on the time-dependent extent of the excited-state electronic wave function throughout the energy-transfer process. The resulting mechanism for the energy-transfer process should be consistent with this picture. Several distinct pathways can be involved, and competition between through-space and through-bond ET mechanisms can take place.[29] The aim of this Letter is to overcome the above-mentioned limitations by treating the dynamics of electronic energy transfer at the atomistic quantum-chemical level and to shed light on the role of environment and temperature effects.

Here we present theoretical results for the dynamics of energy transfer in a molecular dyad system comprising a ladder-type poly(para-phenylene) oligomer donor unit (LPPP5) covalently linked with a perylenemonoimide acceptor unit (PMI) (see Figure 1a). This system has been studied in the past by Singh and Bittner[30] who predicted a kinetic isotope effect using Fermi's golden rule within a harmonic approximation. Ladder-type poly(para-phenylene) are used as hosts in electroluminescent devices[31] and solar cells, whereas perylenes are key components in next-generation solar cells, in particular dye-sensitized cells.[32] Perylene diimide derivatives have also

been used as electron acceptors in bulk heterojunction solar cells with a polymer donor[33] and are promising candidates for fullerene-free organic solar cells.[34,35] Perylene-based chromophores were also found to provide a biomimetic alternative to chlorophyll *a* for use in donor−acceptor systems.[36] Previous work, utilizing single-molecule spectroscopy, has shown that in perylene-end-caped polyindenofluorene chains there is a weak temperature dependence of the energy transfer from the backbone to the end-cap. A much stronger temperature dependence was found for the exciton migration along the polymer backbone,[37] which is consistent with thermally activated diffusion in a landscape of energetically disordered chromophores.[8,38]

In what follows, we use the nonadiabatic excited-state molecular dynamics (NA-ESMD) framework[39,40] to simulate the photoinduced ultrafast intramolecular electronic energy transfer from the LPPP5 donor to the PMI acceptor. NA-ESMD is an efficient *direct* nonadiabatic molecular dynamics simulation method based on the fewest switches surface hopping (FSSH) algorithm originally proposed by Tully.[41] The electronic wave function, expressed in the basis of adiabatic electronic states, is propagated using the time-dependent Schrödinger equation self-consistently with the classical propagation of the nuclei using constant-temperature Langevin dynamics. Electronic excited-state energies, gradients, and nonadiabatic couplings are calculated *on the fly* analytically using the collective electronic oscillator (CEO) approach[42−45] at the configuration interaction singles (CIS) level with the semiempirical Austin model 1 (AM1) Hamiltonian.[46] For excited-state electronic structure of a given molecule in the ground state, the CIS/AM1 results are consistent with that obtained with the time-dependent density functional theory level (LC-wPBE exchange correlation functional and 6-31G* basis set) in terms of the localization pattern of the natural transition orbitals (not shown).

Three different temperature (10, 100, and 300 K) simulations have been performed. For each one, 400 configurations were collected from 1 ns ground-state simulations, thermally equilibrated at their corresponding temperature using a Langevin thermostat with a friction coefficient of 20 ps^{-1} following our previous studies of similar conjugated systems.[47−49] The NA-ESMD simulations were started from these initial configurations by instantaneously promoting the system to the second excited state S_2. A classical time step of 0.5 fs (0.1 fs) has been used for nuclei propagation in ground (nonadiabatic excited) state dynamics. Four time steps per classical step have been used to propagate the electronic wave function during the NA-ESMD. The standard Tully's fewest switches surface hopping algorithm propagates quantum electronic coefficients coherently along each trajectory, without providing any mechanism for dissipating electronic coherence. This results in an internal inconsistency characterized by a disagreement between the fraction of classical trajectories evolving on a given state and the average quantum population for that state. Because of that, a large variety of methods designed to incorporate decoherence in FSSH simulations have been developed. In the present work we adopt the instantaneous decoherence approach previously described and tested for building blocks of phenylene ethynylene dendrimers.[50] Briefly, the method resets the quantum amplitude of the current state to unity after every attempted hop (regardless of whether hops are allowed or forbidden). This simple method is based on the assumption
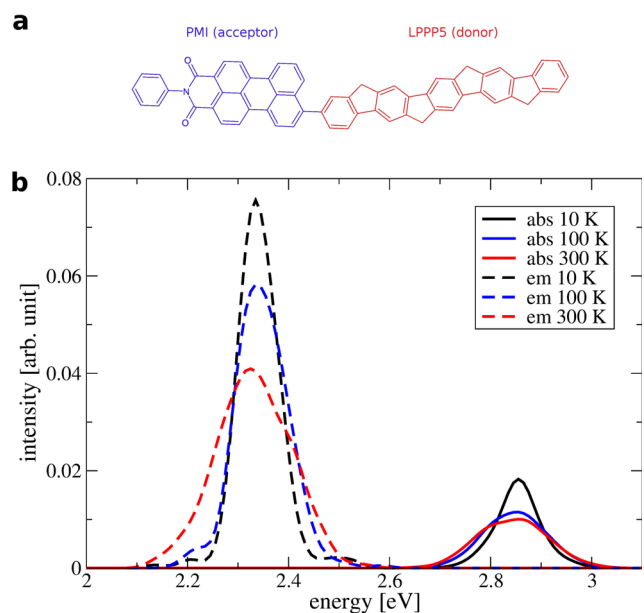

Figure 1. (a) Chemical structure of the LPPP5-PMI dyad and (b) simulated absorption ($S_0 \rightarrow S_2$) and emission ($S_1 \rightarrow S_0$) spectra of LPPP5-PMI at 10, 100, and 300 K.

that wavepackets traveling on different surfaces should immediately separate in phase space and evolve independently. Our previous studies with a variety of combined polyphenylene ethynylene chromophore units have confirmed this feature.[51−53] The approach has been shown to provide qualitative improvement in the agreement between classical and quantum systems at no additional computational cost.

We further analyze the evolution of the dynamics of the trajectory ensemble using transition density matrices reflecting spatial extent of the respective excited states. A quantitative measure of the extent of delocalization of the excitation can be obtained from the participation ratio calculated on the basis of donor, $\rho_{\rm d}$, and acceptor, $\rho_{\rm a}$, transition densities:

$$\mathrm{PR}(t) = (\rho_{\rm d}^2(t) + \rho_{\rm a}^2(t))^{-1}$$

where $\mathrm{PR}(t) \approx 2$ corresponds to transition densities fully delocalized between both donor and acceptor and $\mathrm{PR}(t) \approx 1$ corresponds to complete localization of the transition density on only one moiety. For detailed description of the choice of numerical parameters, the NA-ESMD procedure, and transition density analysis, see refs 39 and 40.

The simulated absorption and emission spectra at 10, 100, and 300 K are shown in Figure 1b. Absorption spectra are calculated from the individual $S_0 \rightarrow S_2$ vertical transition energies and oscillator strengths of the ground-state conformational sampling at the respective temperature, while emission spectra are calculated by averaging the excited-state energies over all trajectories at the end of the nonadiabatic excited-state dynamics, i.e., at 300 fs. The total absorption and fluorescence (accounting for all transitions) is area-normalized to unity. We find that while the absorption spectrum is dominated by the contribution of the S_2 state, the emission takes place from the lowest S_1 excited state. We stress that the broadening of the absorption and fluorescence spectra presented here arises naturally and is purely determined by the conformational fluctuations of the molecule that translate into different absorption and emission energies. These fluctuations are temperature-dependent, leading to a broader distribution with increasing temperature. We find that for absorption, the standard deviation $\sigma = 44$ meV at 10 K, 64 meV at 100 K, and 72 meV at 300 K, while for emission σ varies from 40 meV at 10 K to 51 meV at 100 K and 76 meV at 300 K. Standard deviation values are obtained by fitting a normal distribution to the energy-normalized spectra. We also note that there is negligible spectral overlap between the donor fluorescence and acceptor emission spectra as calculated for the dyad, as shown in the Supporting Information. According to the FRET framework, this would imply inefficient energy transfer from LPPP5 to PMI.

Let us first discuss some universal trends we obtain for the dynamics of energy transfer. Our central result is summarized in Figure 2. After photoexcitation, the molecular system undergoes an ultrafast decay of the initially populated S_2 state (see Figure 2a). This $S_2 \rightarrow S_1$ internal conversion process involves a donor $\rightarrow$ acceptor electronic energy redistribution. This is clearly seen in Figure 2b, where the average fraction of electronic transition density localized on the LPPP5 donor unit ($\rho_{\rm d}$) is displayed. These results suggest that intramolecular electronic ET from the donor LPPP5 to the acceptor PMI unit occurs in the femtosecond time scale with a weak temperature dependence, in clear contradiction to the FRET model. The rate of energy transfer can be estimated by an exponential fit of
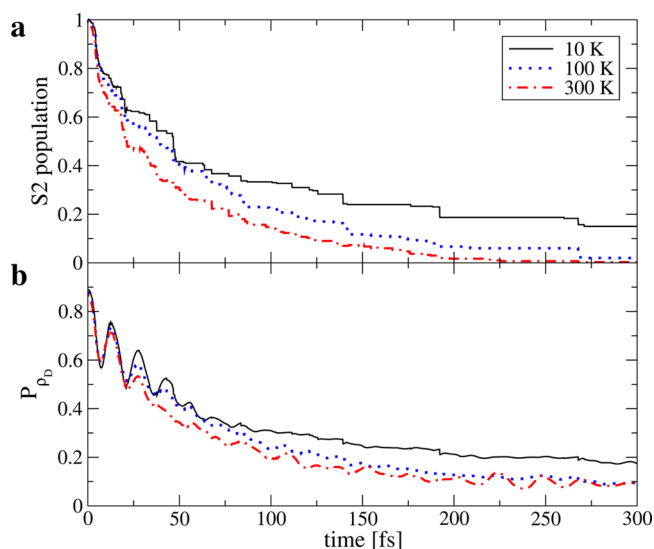

Figure 2. (a) Time-dependence of the average population on S_2 calculated as the fraction of trajectories in this state and (b) time-dependence of the average fraction of electronic transition density localized on the donor LPPP5 unit.

the S_2 population decay at times larger than 5 fs. The obtained value of the relaxation time $\tau \sim 55$ fs at 300 K corresponds to a transfer rate constant $k \sim 18$ ps^{-1}. The value of τ increases to ~ 80 fs by lowering the temperature to 100 K, while at 10 K the relaxation deviates from a monoexponential fit, suggesting that at low temperatures energy relaxation is kinetically hindered (see below). As can be seen in Figure 2, the donor−acceptor energy-transfer process starts during the first 10 fs after initial photoexcitation; hops and attempted hops take place at times earlier than 10 fs. Therefore, the decoherence approach acts from the very beginning of our simulations.

The initial $\rho_{\rm d}$ value ~ 0.9 indicates that the initial excitation to S_2 corresponds to an excess of electronic energy initially localized on the donor LPPP5 unit. Figure 3a shows localization of the electronic transition density of the S_1 and S_2 states at the time of photoexcitation. One can see that S_1 and S_2 states are mainly localized on the acceptor (PMI) and donor (LPPP5) units, respectively. This means that both units are initially uncoupled. Nevertheless, nuclear motion on the S_2 state rapidly mixes electronic states providing ultrafast donor $\rightarrow$ acceptor energy transfer. Figure 3a also depicts the localization of the electronic transition density of the S_1 and S_2 states at ~ 5 fs after photoexcitation. A complete delocalization between both units can be seen, indicating a strong interaction between the states. The time evolution of the participation ratio during the NA-ESMD simulations at different temperatures is plotted in Figure 3b. The ultrafast increase of $\mathrm{PR}(t)$ during the first ~ 5 fs indicates an ultrafast spatial delocalization of the excitation. Furthermore, large values of $\mathrm{PR}(t)$ persist during ~ 100 fs after photoexcitation. These results indicate that the average values of $\rho_{\rm d}$ reported in Figure 2 do not represent a spatial scrambling due to hopping between donor and acceptor sites, but rather a transient delocalization of the wave function between both units. This partially delocalized character of the excited state over the donor and acceptor units can explain our faster relaxation times compared with previous calculated golden-rule rates by Singh and Bittner.[30] The interaction between S_2 (initially localized on the donor unit) and S_1 (initially localized on the acceptor unit) states is revealed in
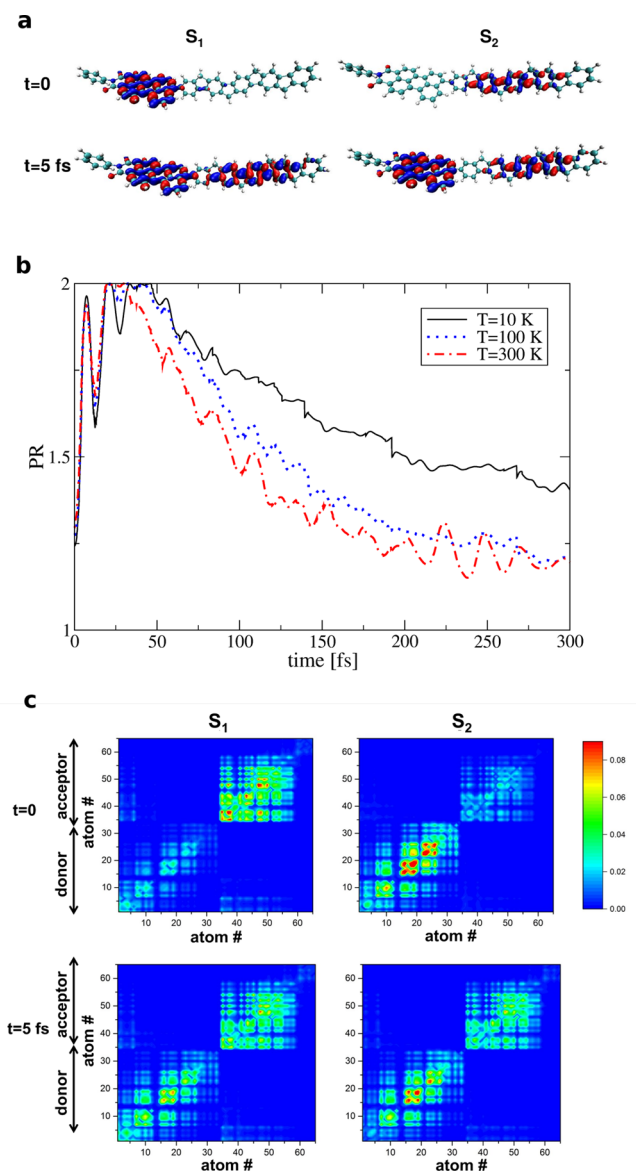
Figure 3. (a) Localization of the electronic transition densities for S_2 and S_1 states at initial times and at ~5 fs after photoexcitation; (b) time-dependence of the average participation ratio; and (c) two-dimensional plots of transition density matrix elements for the S_1 and S_2 state, on the basis of donor and acceptor atomic orbitals, at $t = 0$ and at the moment of $S_2 \rightarrow S_1$ quantum transition (5.7 fs) for a typical trajectory at 300 K. The x and y axes denote spatial positioning of an electron and a hole in respective atomic orbitals for atoms ordered along the molecular backbone. The color coding is shown on the side. Block diagonal quadrants correspond to localized excitation on the donor (lower quadrant) or the acceptor (upper quadrant) units, while diagonal blocks correspond to charge-transfer contributions.

the ultrafast increase of the nonadiabatic coupling (see Figure 4b), reaching a maximum in ~5 fs. Both states remain coupled for the first 100 fs after photoexcitation. The above transient delocalization scenario can be easily visualized in the video file of the time evolution of the transition density fluctuations during the dynamics for a representative trajectory, included in the Supporting Information file.

This delocalization of electronic wave function pronounced in the orbital plots (Figure 3a) potentially assumes two distinct scenarios triggering quantum transition and thus an energy-
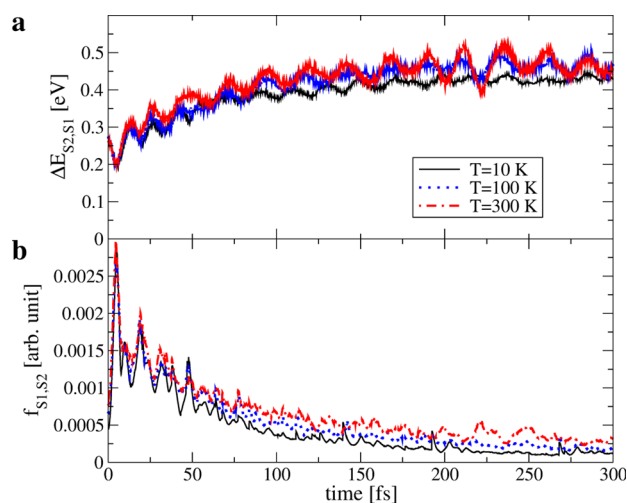

Figure 4. (a) Time dependence of the average energy gap, ΔE, between the S_2 and the S_1 states and (b) time dependence of the average nonadiabatic couplings.

transfer event. In the first one, energetic quasi-degeneracy of S_2 (donor unit) and S_1 (acceptor unit) electronic level leads to quantum superposition of these coupled states. This picture, known as a Frenkel exciton, assumes that the electron−hole pair is spatially located on either donor or acceptor unit with no charge-transfer contribution. In the opposite limit, the charge-transfer processes are allowed, where an electron and a hole occupy different units. To delineate between these cases, we further invoke an analysis of the entire transition density matrix (TDM) in real-space.[40,42,43] Notably, that orbital plots in Figure 3a reflect spatial positioning of only diagonal elements of TDM. The respective two-dimensional plot of the TDMs of S_1 and S_2 states at $t = 0$ and $t \sim 5$ fs after photoexcitation are shown in Figure 3c. Concomitant to the orbital plots, initially at $t = 0$, the wave functions of S_1 and S_2 states are delocalized over the lower and upper diagonal quadrants corresponding to the acceptor and donor units, respectively. We observe very minor cross-delocalization. The situation changes at the moment of quantum transition at $t = 5$ fs after photoexcitation: both S_1 and S_2 states become uniformly delocalized across the entire molecule, occupying the diagonal blocks only. It is very important that amplitudes of the off-diagonal quadrants indicating charge-transfer character between the donor and acceptor (i.e., positioning of the electron and the hole on different units) remain negligible in all case. Thus, this analysis clearly emphasizes a dominance of the Frenkel character of the excitation during the course of the energy-transfer event. The molecular dyad considered here cannot be considered fully conjugated as there is a torsion angle between the donor and acceptor units of about 58°. Therefore, we do not observe a charge-transfer character in electronic excitations during dynamics.

At this point it is interesting to note that the $S_2 \rightarrow S_1$ internal conversion process seems to be temperature-independent during the first ~5 fs of excited-state dynamics: an ultrafast decay of S_2 population (Figure 2a), concomitant with a fast electronic transition density delocalization (Figures 2b and 3b). The reason behind it can be found in the analysis of the time evolution of the energy gap, ΔE, between both states. According to the Hellmann−Feynman theorem, the non-adiabatic coupling scales as $1/\Delta E$. Therefore, large nonadiabatic couplings are expected while the molecular system undergoes

regions with a small energy gap. Figure 4 presents the time evolution of the average ΔE_{12} between the S_2 and S_1 states. A first minimum is reached during the first $\sim$5 fs, with a consequent ultrafast increase of the nonadiabatic coupling between both units (Figure 4b). The initial nuclear forces on S_2 efficiently lead the system to regions of the phase-space described by significant delocalization of the electronic wave function between the donor and acceptor units (Figure 3b) that drives quantum mechanical level repulsion. This initial effect is temperature independent. After that, the system moves to regions of low nonadiabatic coupling until it finally undergoes a second region of large nonadiabatic coupling and small energy gap at $\sim$20 fs. Nevertheless, this latter process is less pronounced and weakly temperature-dependent. This behavior is repeated during the first $\sim$50 fs of simulations, becoming even less marked over time. As a result, oscillations involving changes in the localization of the excitation take place during that time window (see Figure 2b). During energy relaxation, high-frequency modes make the molecular system experience successive crossings through the region of the configuration space with small energy gap (Figure 4a) and, therefore, strong couplings (Figure 4b). As a consequence, oscillations in the localization of transition density are observed (Figure 2b). At later times, once the S_1 state becomes significantly populated, the molecular system remains in regions of the conformational space characterized by low nonadiabatic couplings (Figure 4b), large separation between states (Figure 4a), and electronic wave function localization on the acceptor unit (Figure 3c). That is, nuclear motions on S_1 state decouples donor and acceptor units.

We have also investigated the role of the environment on the energy-transfer dynamics. This is taken into account through the friction coefficient in the Langevin equation that represents the interaction of the atoms with the environment bath. The value of the friction coefficient determines the absolute time scale for the energy relaxation process. A low value of γ characterizes a system with a weak hydrodynamic drag, i.e., weak interactions with the solvent, for example when the molecule is embedded in an aqueous solution, whereas when the value of γ is increased, the environment progressively plays a more important role, taking the system to the strong damping, Smoluchowski regime for very large values of γ.[54] We have allowed the γ parameter to vary from 2 to 200 ps^{-1}. In the low-friction regime, for $\gamma = 2$ ps^{-1}, we find that the temperature dependence of ET is almost negligible while increasing γ progressively decreases the ET rate, in particular at low temperatures (see the Supporting Information). At 10 K, for $\gamma = 2$ ps^{-1} the half-life ($t_{1/2}$) of the S_2 population is $\sim$46 fs whereas for $\gamma = 200$ ps^{-1}, $t_{1/2}$ increases to $\sim$192 fs. Increasing γ results in lower nuclear velocities and therefore lower nonadiabatic couplings. Larger viscosity overdamps nuclear relaxation. Recurrences in the average ΔE_{12}, observed at low γ values, disappear as γ increases because of dephasing and solvent friction (see the Supporting Information). Consequently, the conformational space is sampled at a slower pace for large γ values, leading to less effective couplings between both states.

In conclusion, we have studied the ultrafast donor $\rightarrow$ acceptor intramolecular energy transfer in the model LPPP5-PMI dyad system by using atomistic NA-ESMD simulations. Despite the rather temperature-independent initial donor $\rightarrow$ acceptor energy funneling, the entire internal conversion process presents a weak temperature dependence

case, concomitant with the lack of direct overlap between a donor emission and an acceptor absorption lineshapes at any temperature. Significant changes and fluctuations in the (de)localization of the electronic transition density are observed during the process of energy transfer. While the excitation is initially localized on the donor moiety, it rapidly becomes fully delocalized over the whole dyad because of gradients on the S_2 state presenting transient fluctuations between both moieties. At latter times, while the electronic population relaxes on the S_1 state, the excitation evolution ends by getting trapped on the acceptor unit. We consequently find that energy transfer cannot be described by a Förster mechanism, and our results qualitatively agree with single-molecule spectroscopic experiments in similar systems. For example, ultrafast ET time scales have been reported in short bridge connected perylenediimide–terrylenediimide molecular dyads at low temperatures[22] as well as at room temperature in aminopyrenyl–aminobenzanthronyl bichromophores[55] and benzothiazole–borondipyrromethene donor–acceptor dyads.[56] This rapid delocalization of electronic excitation at the moment of quantum transition does not include charge-transfer contributions, which places such excitations at the Frenkel-type exciton limit. Overall, our results suggest that molecular design of efficient energy donor–acceptors molecular materials can take advantage of through-bond energy-transfer mechanisms assisted by pronounced delocalization processes.

■ ASSOCIATED CONTENT

ⓢ Supporting Information

The Supporting Information is available free of charge on the ACS Publications website at DOI: 10.1021/acs.jpclett.7b00259.

> Spectra and plots of time dependence of S_2 population, nonadiabatic couplings, and energy gaps (PDF)
> Video of the transition density dynamics (AVI)

■ AUTHOR INFORMATION

Corresponding Author
*E-mail: astavros@fis.uc3m.es.

ORCID ⓘ
Stavros Athanasopoulos: 0000-0003-0753-2643

Notes
The authors declare no competing financial interest.

■ ACKNOWLEDGMENTS

■ REFERENCES

(1) Scholes, G. D. Long-Range Resonance Energy Transfer in Molecular Systems. *Annu. Rev. Phys. Chem.* **2003**, *54*, 57−87.

(2) Shihong, L.; Fang, G.; Yimeng, G.; Ying, H.; Hongru, L.; Shengtao, Z. Photoinduced Intramolecular Energy Transfer in Dendrimers. *Prog. Chem.* **2010**, *22*, 2033−2052.

(3) McConnell, I.; Li, G.; Brudvig, G. W. Energy Conversion in Natural and Artificial Photosynthesis. *Chem. Biol.* **2010**, *17*, 434−447.

(4) Blankenship, R. E. *Molecular Mechanisms of Photosynthesis*; Blackwell Science Ltd: Oxford, U.K., 2008.

(5) Ziessel, R.; Harriman, A. Artificial light-harvesting antennae: electronic energy transfer by way of molecular funnels. *Chem. Commun.* **2011**, *47*, 611−631.

(6) Askim, J. R.; Mahmoudi, M.; Suslick, K. S. Optical sensor arrays for chemical sensing: the optoelectronic nose. *Chem. Soc. Rev.* **2013**, *42*, 8649−8682.

(7) Ostroverkhova, O. Organic Optoelectronic Materials: Mechanisms and Applications. *Chem. Rev.* **2016**, *116*, 13279−13412.

(8) Athanasopoulos, S.; Emelianova, E. V.; Walker, A. B.; Beljonne, D. Exciton diffusion in energetically disordered organic materials. *Phys. Rev. B: Condens. Matter Mater. Phys.* **2009**, *80*, 195209.

(9) Mikhnenko, O. V.; Blom, P. W. M.; Nguyen, T.-Q. Exciton diffusion in organic semiconductors. *Energy Environ. Sci.* **2015**, *8*, 1867−1888.

(10) Athanasopoulos, S.; Hennebicq, E.; Beljonne, D.; Walker, A. B. Trap limited exciton transport in conjugated polymers. *J. Phys. Chem. C* **2008**, *112*, 11532−11538.

(11) Kuik, M.; Wetzelaer, G.-J. A. H.; Nicolai, H. T.; Craciun, N. I.; De Leeuw, D. M.; Blom, P. W. M. 25th Anniversary Article: Charge Transport and Recombination in Polymer Light-Emitting Diodes. *Adv. Mater.* **2014**, *26*, 512−531.

(12) Krueger, B. P.; Scholes, G. D.; Fleming, G. R. Calculation of Couplings and Energy-Transfer Pathways between the Pigments of LH2 by the ab Initio Transition Density Cube Method. *J. Phys. Chem. B* **1998**, *102*, 5378−5386.

(13) Ortiz, W.; Krueger, B. P.; Kleiman, V. D.; Krause, J. L.; Roitberg, A. E. Energy Transfer in the Nanostar: The Role of Coulombic Coupling and Dynamics. *J. Phys. Chem. B* **2005**, *109*, 11512−11519.

(14) Tretiak, S.; Middleton, C.; Chernyak, V.; Mukamel, S. Bacteriochlorophyll and Carotenoid Excitonic Couplings in the LH2 System of Purple Bacteria. *J. Phys. Chem. B* **2000**, *104*, 9540−9553.

(15) Hennebicq, E.; Beljonne, D.; Curutchet, C.; Scholes, G. D.; Silbey, R. J. Shared-mode assisted resonant energy transfer in the weak coupling regime. *J. Chem. Phys.* **2009**, *130*, 214505.

(16) Kleima, F. J.; Hofmann, E.; Gobets, B.; van Stokkum, I. H. M.; van Grondelle, R.; Diederichs, K.; van Amerongen, H. Förster Excitation Energy Transfer in Peridinin-Chlorophyll-a-Protein. *Biophys. J.* **2000**, *78*, 344−353.

(17) Young, A. J.; Frank, H. A. Energy transfer reactions involving carotenoids: quenching of chlorophyll fluorescence. *J. Photochem. Photobiol., B* **1996**, *36*, 3−15.

(18) Pullerits, T.; Hess, S.; Herek, J. L.; Sundström, V. Temperature Dependence of Excitation Transfer in LH2 of Rhodobacter sphaeroides. *J. Phys. Chem. B* **1997**, *101*, 10560−10567.

(19) Sundström, V.; Pullerits, T.; van Grondelle, R. Photosynthetic Light-Harvesting: Reconciling Dynamics and Structure of Purple Bacterial LH2 Reveals Function of Photosynthetic Unit. *J. Phys. Chem. B* **1999**, *103*, 2327−2346.

(20) Beljonne, D.; Curutchet, C.; Scholes, G. D.; Silbey, R. J. Beyond Förster Resonance Energy Transfer in Biological and Nanoscale Systems. *J. Phys. Chem. B* **2009**, *113*, 6583−6599.

(21) Becker, K.; Lupton, J. M.; Feldmann, J.; Setayesh, S.; Grimsdale, A. C.; Müllen, K. Efficient Intramolecular Energy Transfer in Single Endcapped Conjugated Polymer Molecules in the Absence of Appreciable Spectral Overlap. *J. Am. Chem. Soc.* **2006**, *128*, 680−681.

(22) Hinze, G.; Métivier, R.; Nolde, F.; Müllen, K.; Basché, T. Intramolecular electronic excitation energy transfer in donor/acceptor dyads studied by time and frequency resolved single molecule spectroscopy. *J. Chem. Phys.* **2008**, *128*, 124516.

(23) Marguet, S.; Markovitsi, D.; Millié, P.; Sigal, H.; Kumar, S. Influence of Disorder on Electronic Excited States: An Experimental and Numerical Study of Alkylthiotriphenylene Columnar Phases. *J. Phys. Chem. B* **1998**, *102*, 4697−4710.

(24) Beljonne, D.; Cornil, J.; Silbey, R.; Millie, P.; Bredas, J. L. Interchain interactions in conjugated materials: The exciton model versus the supermolecular approach. *J. Chem. Phys.* **2000**, *112*, 4749−4758.

(25) Dexter, D. L. A Theory of Sensitized Luminescence in Solids. *J. Chem. Phys.* **1953**, *21*, 836−850.

(26) Sternlicht, H.; Nieman, G. C.; Robinson, G. W. Triplet—Triplet Annihilation and Delayed Fluorescence in Molecular Aggregates. *J. Chem. Phys.* **1963**, *38*, 1326−1335.

(27) Colson, S. D.; Robinson, G. W. Trap—Trap Triplet Energy Transfer in Isotopic Mixed Benzene Crystals. *J. Chem. Phys.* **1968**, *48*, 2550−2556.

(28) Nalbach, P.; Pugliesi, I.; Langhals, H.; Thorwart, M. Noise-Induced Förster Resonant Energy Transfer between Orthogonal Dipoles in Photoexcited Molecules. *Phys. Rev. Lett.* **2012**, *108*, 218302.

(29) Fernandez-Alberti, S.; Roitberg, A. E.; Kleiman, V. D.; Nelson, T.; Tretiak, S. Shishiodoshi unidirectional energy transfer mechanism in phenylene ethynylene dendrimers. *J. Chem. Phys.* **2012**, *137*, 22A526.

(30) Singh, J.; Bittner, E. R. Isotopic effect and temperature dependent intramolecular excitation energy transfer in a model donor-acceptor dyad. *Phys. Chem. Chem. Phys.* **2010**, *12*, 7418−7426.

(31) Yang, X. H.; Neher, D.; Scherf, U.; Bagnich, S. A.; Bässler, H. Polymer electrophosphorescent devices utilizing a ladder-type poly-(para-phenylene) host. *J. Appl. Phys.* **2003**, *93*, 4413−4419.

(32) Li, C.; Wonneberger, H. Perylene Imides for Organic Photovoltaics: Yesterday, Today, and Tomorrow. *Adv. Mater.* **2012**, *24*, 613−636.

(33) Howard, I. A.; Laquai, F.; Keivanidis, P. E.; Friend, R. H.; Greenham, N. C. Perylene Tetracarboxydiimide as an Electron Acceptor in Organic Solar Cells: A Study of Charge Generation and Recombination. *J. Phys. Chem. C* **2009**, *113*, 21225−21232.

(34) Singh, R.; Aluicio-Sarduy, E.; Kan, Z.; Ye, T.; MacKenzie, R. C. I.; Keivanidis, P. E. Fullerene-free organic solar cells with an efficiency of 3.7% based on a low-cost geometrically planar perylene diimide monomer. *J. Mater. Chem. A* **2014**, *2*, 14348−14353.

(35) Ye, L.; Sun, K.; Jiang, W.; Zhang, S.; Zhao, W.; Yao, H.; Wang, Z.; Hou, J. Enhanced Efficiency in Fullerene-Free Polymer Solar Cell by Incorporating Fine-designed Donor and Acceptor Materials. *ACS Appl. Mater. Interfaces* **2015**, *7*, 9274−9280.

(36) Lukas, A. S.; Zhao, Y.; Miller, S. E.; Wasielewski, M. R. Biomimetic Electron Transfer Using Low Energy Excited States: A Green Perylene-Based Analogue of Chlorophyll a. *J. Phys. Chem. B* **2002**, *106*, 1299−1306.

(37) Becker, K.; Lupton, J. M. Efficient Light Harvesting in Dye-Endcapped Conjugated Polymers Probed by Single Molecule Spectroscopy. *J. Am. Chem. Soc.* **2006**, *128*, 6468−6479.

(38) Athanasopoulos, S.; Hoffmann, S. T.; Bässler, H.; Köhler, A.; Beljonne, D. To Hop or Not to Hop? Understanding the Temperature Dependence of Spectral Diffusion in Organic Semiconductors. *J. Phys. Chem. Lett.* **2013**, *4*, 1694−1700.

(39) Nelson, T.; Fernandez-Alberti, S.; Roitberg, A. E.; Tretiak, S. Nonadiabatic Excited-State Molecular Dynamics: Modeling Photophysics in Organic Conjugated Materials. *Acc. Chem. Res.* **2014**, *47*, 1155−1164.

(40) Nelson, T.; Fernandez-Alberti, S.; Chernyak, V.; Roitberg, A. E.; Tretiak, S. Nonadiabatic Excited-State Molecular Dynamics Modeling of Photoinduced Dynamics in Conjugated Molecules. *J. Phys. Chem. B* **2011**, *115*, 5402−5414.

(41) Tully, J. C. Molecular dynamics with electronic transitions. *J. Chem. Phys.* **1990**, *93*, 1061−1071.

(42) Mukamel, S.; Tretiak, S.; Wagersreiter, T.; Chernyak, V. Electronic Coherence and Collective Optical Excitations of Conjugated Molecules. *Science* **1997**, *277*, 781−787.

(43) Tretiak, S.; Chernyak, V.; Mukamel, S. Recursive density-matrix-spectral-moment algorithm for molecular nonlinear polarizabilities. *J. Chem. Phys.* **1996**, *105*, 8914−8928.

(44) Tretiak, S.; Zhang, W. M.; Chernyak, V.; Mukamel, S. Excitonic couplings and electronic coherence in bridged naphthalene dimers. *Proc. Natl. Acad. Sci. U. S. A.* **1999**, *96*, 13003−13008.

(45) Tretiak, S.; Mukamel, S. Density Matrix Analysis and Simulation of Electronic Excitations in Conjugated and Aggregated Molecules. *Chem. Rev.* **2002**, *102*, 3171−3212.

(46) Dewar, M. J. S.; Zoebisch, E. G.; Healy, E. F.; Stewart, J. J. P. Development and use of quantum mechanical molecular models. 76. AM1: a new general purpose quantum mechanical molecular model. *J. Am. Chem. Soc.* **1985**, *107*, 3902−3909.

(47) Alfonso Hernandez, L.; Nelson, T.; Tretiak, S.; Fernandez-Alberti, S. Photoexcited Energy Transfer in a Weakly Coupled Dimer. *J. Phys. Chem. B* **2015**, *119*, 7242−7252.

(48) Alfonso Hernandez, L.; Nelson, T.; Gelin, M. F.; Lupton, J. M.; Tretiak, S.; Fernandez-Alberti, S. Interference of Interchromophoric Energy-Transfer Pathways in π-Conjugated Macrocycles. *J. Phys. Chem. Lett.* **2016**, *7*, 4936−4944.

(49) Galindo, J. F.; Atas, E.; Altan, A.; Kuroda, D. G.; Fernandez-Alberti, S.; Tretiak, S.; Roitberg, A. E.; Kleiman, V. D. Dynamics of Energy Transfer in a Conjugated Dendrimer Driven by Ultrafast Localization of Excitations. *J. Am. Chem. Soc.* **2015**, *137*, 11637−11644.

(50) Nelson, T.; Fernandez-Alberti, S.; Roitberg, A. E.; Tretiak, S. Nonadiabatic excited-state molecular dynamics: Treatment of electronic decoherence. *J. Chem. Phys.* **2013**, *138*, 224111.

(51) Fernandez-Alberti, S.; Kleiman, V. D.; Tretiak, S.; Roitberg, A. E. Unidirectional Energy Transfer in Conjugated Molecules: The Crucial Role of High-Frequency C≡C Bonds. *J. Phys. Chem. Lett.* **2010**, *1*, 2699−2704.

(52) Fernandez-Alberti, S.; Kleiman, V. D.; Tretiak, S.; Roitberg, A. E. Nonadiabatic Molecular Dynamics Simulations of the Energy Transfer between Building Blocks in a Phenylene Ethynylene Dendrimer. *J. Phys. Chem. A* **2009**, *113*, 7535−7542.

(53) Galindo, J. F.; Fernandez-Alberti, S.; Roitberg, A. E. Electronic Excited State Specific IR Spectra for Phenylene Ethynylene Dendrimer Building Blocks. *J. Phys. Chem. C* **2013**, *117*, 26517−26528.

(54) Schuss, Z. Brownian Simulation of Langevin's. In *Brownian Dynamics at Boundaries and Interfaces: In Physics, Chemistry, and Biology*; Springer: New York, 2013; pp 89−109.

(55) Dvorak, M.; Fidler, V.; Lohse, P. W.; Michl, M.; Oum, K.; Wagener, P.; Schroeder, J. Ultrafast intramolecular electronic energy transfer in rigidly linked aminopyrenyl-aminobenzanthronyl dyads-a femtosecond study. *Phys. Chem. Chem. Phys.* **2009**, *11*, 317−323.

(56) Badgurjar, D.; Sudhakar, K.; Jain, K.; Kalantri, V.; Venkatesh, Y.; Duvva, N.; Prasanthkumar, S.; Sharma, A. K.; Bangal, P. R.; Chitta, R.; Giribabu, L. Ultrafast Intramolecular Photoinduced Energy Transfer Events in Benzothiazole−Borondipyrromethene Donor−Acceptor Dyads. *J. Phys. Chem. C* **2016**, *120*, 16305−16321.